BRADLEY
University

Senior Capstone Project Proposal

Battery Electrochemical Impedance Spectroscopy Board

Team:
Will Anderson

Advisor:
Dr. Brian Huggins

26 November 2018

Table of Contents

I. **Introduction……………………………………………………………………………....……2**

II. **Problem Statement…………………………………………………………………...….…..2**

III. **Review of Electrochemical Impedance Spectroscopy……………………...………………..2**

IV. **Functional Description………………………………………………………….….….……4**

V. **Technical Specifications……………………………………………….………...………7**

a. **AD5933**

b. **AD5174**

VI. **Schedule…...……………………………………………………………….…...….….10**

VII. **References…...…………………………………………...…………………………...……11**

I. Introduction

The battery market is one of the fastest growing markets in recent years as we are becoming more and more dependent on technologies that rely on battery storage. Consequently, there is a need for the performance of these rechargeable batteries to be as efficient and reliable as fundamentally possible. The two most common metrics for measuring the capabilities of a battery are state of charge (SOC) and state of health (SOH). The SOC metric reports the amount of energy remaining in the battery as compared to when the battery was at it maximum energy potential. The SOH metric, ideally, is a subjective method able to inform the battery user with the overall condition and performance capabilities to be expected of the battery.

However, there is a great deal of uncertainty associated with being able to accurately report the SOH of a battery over its lifetime as there is no universal definition of SOH. Many of the current SOH solutions require bulky and expensive equipment that is not viable for use on most battery management systems. As a result, a lightweight, compact, low power, and inexpensive solution must be found for a real-time SOH monitor to be attached to a deployable battery.

II. Problem Statement

Through an extensive review of relevant literature, it has been determined that Electrochemical Impedance Spectroscopy (EIS) is the most effective solution for characterizing the performance of batteries. The basic principle of EIS is to input an excitation signal into the battery and observe the characteristic response. The proper implementation of EIS on board in real-time would greatly improve the overall effectiveness of a battery management system by: enhancing accuracy of SOC and SOH measurements, fine tuning individual cell balancing, extending discharge cycles, shortening charge cycles, and second life benefits. Consequently, Sandia National Laboratories has created an EIS board that utilizes the AD5933 impedance analyzer to excite a battery and characterize the impedance response on board and in real time.

My objective moving forward in this project will be to write all of the firmware for this EIS board, debug and ensure performance of all of the hardware, and have the system functioning at a level capable of retrieving the impedance data from a power supply or battery simulator.

III. Review of Electrochemical Impedance Spectroscopy

In real world circuits, there exists more than just electrical resistance that opposes the flow of the electrical current. These circuits possess a more complex and general circuit parameter known as impedance. Impedance can be defined similarly to resistance as the ability of a circuit to resist the flow of the current in the system. However, impedance differs from resistance in ways such as: impedance does not follow Ohm's law at all voltage and current levels, impedance is dependent on frequency, and the AC current and voltage will not be in phase with each other.

Electrochemical impedance is typically found by exciting an electrochemical cell with a small sinusoidal (AC) and measuring the generated response. For instance, a small sinusoidal current input will yield an approximately sinusoidal voltage response due to the linearity of the system, with a shift in phase. The complex impedance can be calculated as the ratio between the voltage and current at a specific frequency: $Z(w) = \frac{V(w)}{I(W)}$

This complex impedance can be broken into two parts: real and imaginary impedance. The magnitude and phase of the impedance can also be useful parameters in characterizing the battery. The spectroscopy part of EIS can be obtained by performing the measurement described above for many frequencies, creating an impedance spectrum. This is the function of the AD5933 impedance converter and network analyzer described later in this document.

Furthermore, EIS offers a wealth of information on battery systems and can be used to track changes in battery health characteristics under various storage or usage conditions. Application of EIS on battery systems include and are not limited to: analysis of state of charge, study of reaction mechanisms, change of active surface area during operation, separator evaluation, passivating film behavior, separation and comparison of electrode kinetics on each electrode, identification of possible corrosion processes, and investigation of the kinetics at each electrode. For our purposes, we will be utilizing EIS to generate frequency response and Nyquist curves from the complex impedance that is calculated on board and in real time with the objective of obtaining data that is similar with the established results for this procedure on computerized simulations.

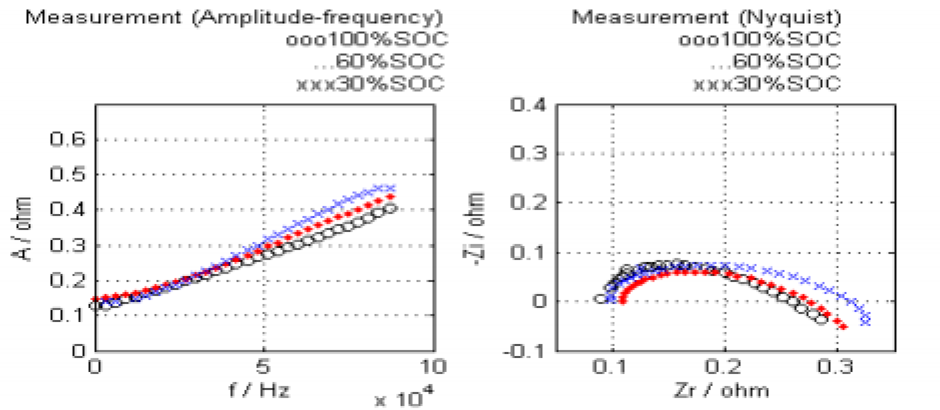

Figure 1: Frequency Response and Nyquist Plots [5]

IV. Functional Description

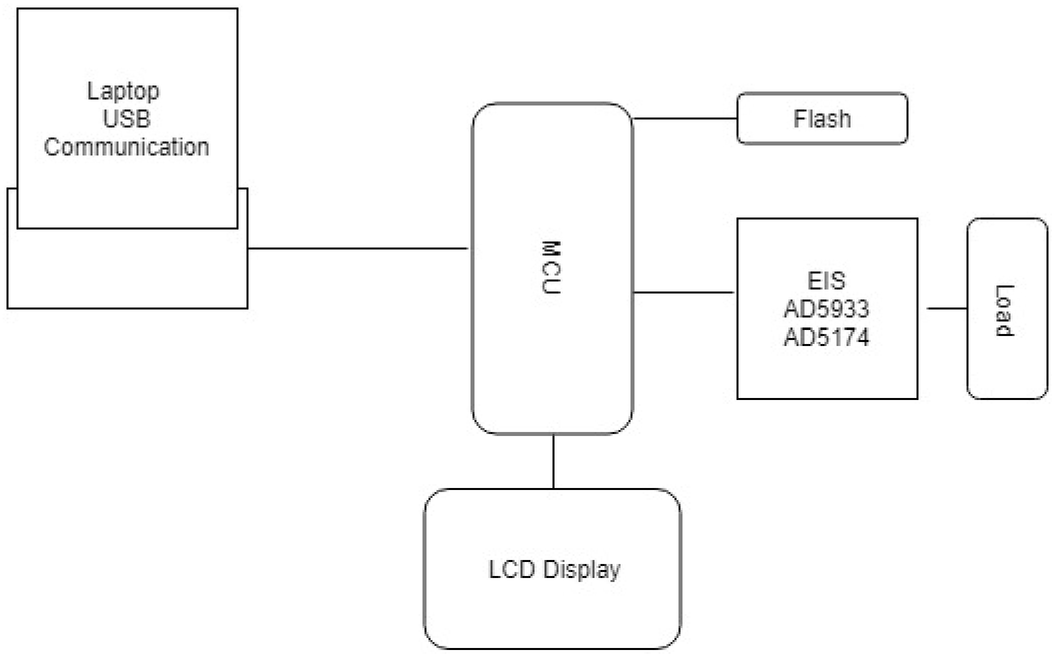

Figure 2: High Level EIS Block Diagram

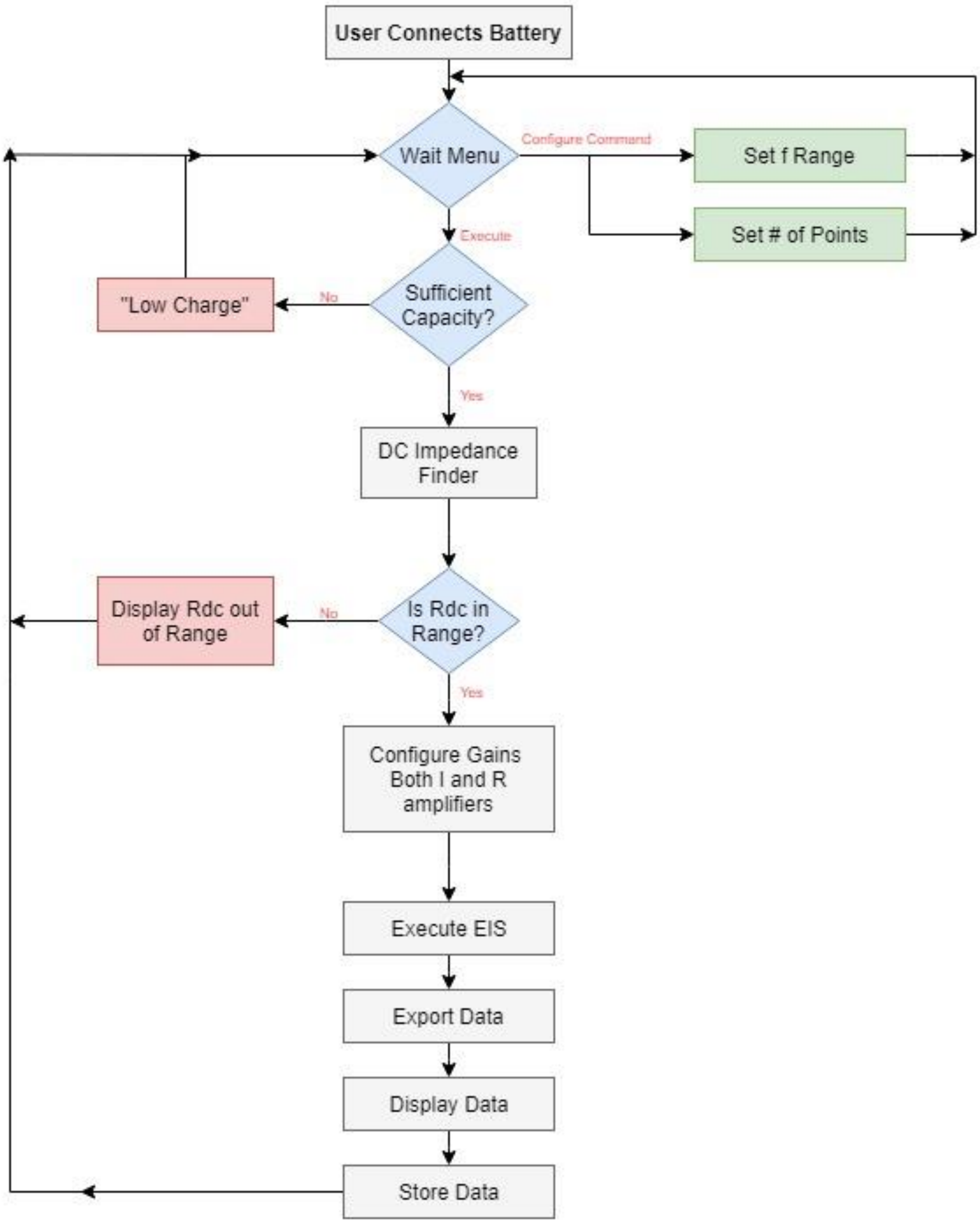

Figure 3: EIS Software Functionality Block Diagram

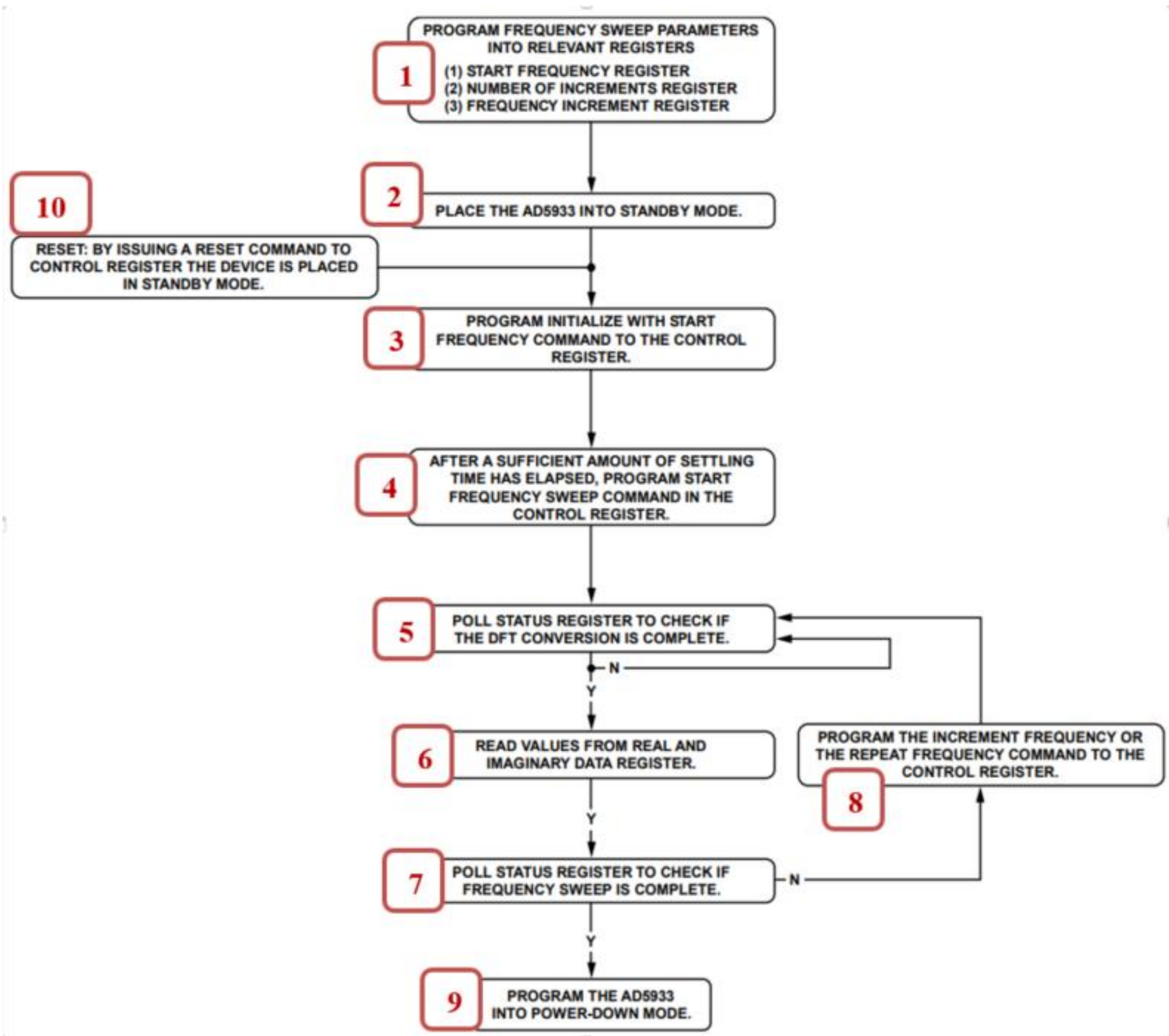

Figure 4: Process of Programming the AD5933

V. Technical Specifications

A. AD5933 [28]

Features Summary:

- Programmable output p2p excitation voltage to a maximum frequency of 100 kHz
- Programmable frequency sweep capability with serial I2C interface
- Frequency resolution of 27 bits (<0.1 Hz)
- Impedance measurement range from 1 kΩ to 10 MΩ
- Capable of measuring of 100 Ω to 1 kΩ with additional circuitry
- Internal temperature sensor (±2°C)
- Internal system clock option
- Phase measurement capability
- System accuracy of 0.5%
- 2.7 V to 5.5 V power supply operation
- Temperature range: −40°C to +125°C
- 16-lead SSOP package
- Qualified for automotive applications

General Notes:

- Combines on board frequency generator with 12 bit ADC
- Allows for external impedance to be excited by known frequency
- ADC samples the response from impedance
- DFT of response is performed by on-board DSP engine
- Needs calibration for accurate use
- Needs extra buffer circuitry for impedance 100Ω -1 kΩ

Additional Notes:

- We will need to figure out how long the initial settling time needs to be, which I expect to be driven by the response of the battery as well as the AC coupling filter to the input of the ripple sense amplifier, which has an RC time constant of 0.484s (it was required to be this slow so that it works down to 10Hz)
- AD5933 defaults into power-down mode (0xA000)
- AD5933 can also measure temperature
- AD5174 also has permanent memory that stores 50 set points (loops through each point, can only be written to once)
- We will need to calibrate at whatever ranges we want to determine the gain factor (for calculating the actual impedance for the real and imaginary data in the registers).
- Possible use of internal clock if frequency accuracy is not essential

Summary of Gains:

- AD5933 output amplitude options: 0.198, 0.383, 0.97, 1.98 $V_{pk\text{-}pk}$ (~3% tolerance) (corresponds to output offset options of 0.173, 0.31, 0.76, 1.48V).
- This is then multiplied by 0.6 (buffered voltage divider with 1% resistors). This is then converted to a current through the battery by a transimpedance amplifier with a gain of 2A/V (1%)

- Overall transimpedance gain from the AD5933 output to the current through the battery is 1.2A/V.
- The battery voltage ripple is AC coupled to the AD8421 instrumentation amplifier, whose gain is set by the AD5174 10-bit 10kΩ rheostat. The gain of the amplifier is $G = 1 + \frac{9.9k\Omega}{R_G}$, where R_G is the resistance of the rheostat, which makes the gain $G = 1 + \frac{9.9k\Omega}{10k\Omega \cdot \frac{D}{2^{10}} R_G} = 1 + \frac{0.99 \cdot 2^{10}}{D \cdot R_G}$, where D is the value of the AD5174 RDAC wiper register. The amplified signal is then amplified by the programmable gain amplifier inside the AD5933 by a factor of 5x or 1x.

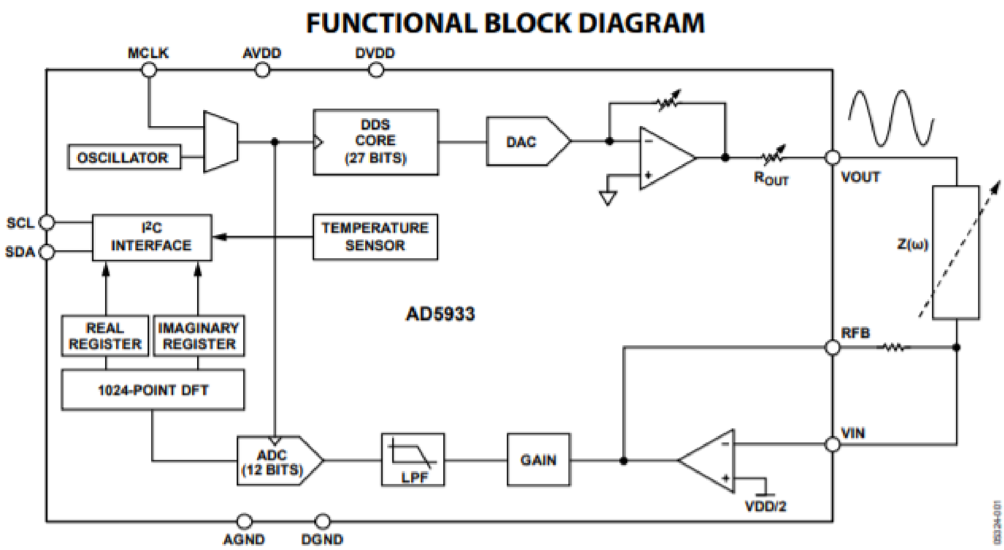

Figure 5: AD5933 Block Diagram

Usage Notes:

- Frequency (f) sweep is performed with user-defined start f, f resolution, number of points.
- DFT for each point in the sweep. The multiplication is accumulated over 1024 samples for each individual frequency point. Two 16-bit registers will hold the real and imaginary parts of the result in twos complement format.
- Impedance calculation done by taking magnitude of real and imaginary parts

Example Usage of AD5933 [5]:

- Combines AD5933 with ARM controller and peripheral circuitry to do EIS.

- Our main point of difference from this work is that they do all of their post-processing on a computer whereas we want to do ours on board to be able to send the State of Health metric back to the user in real-time.
- Their design was also too bulky for our applications so our board design is in a more fitting form factor.
- If we can get on-board results to match that of this paper's experimental data then we know we are on the right track.

B. AD5174 [29]

Features Summary:

- 50-times programmable wiper memory
- SPI-compatible interface
- Single-channel, 1024-position resolution
- Nonvolatile memory in compact package

General Applications:

- Mechanical rheostat replacements
- Variable gain control
- Programmable voltage to current conversions
- Sensor Calibration

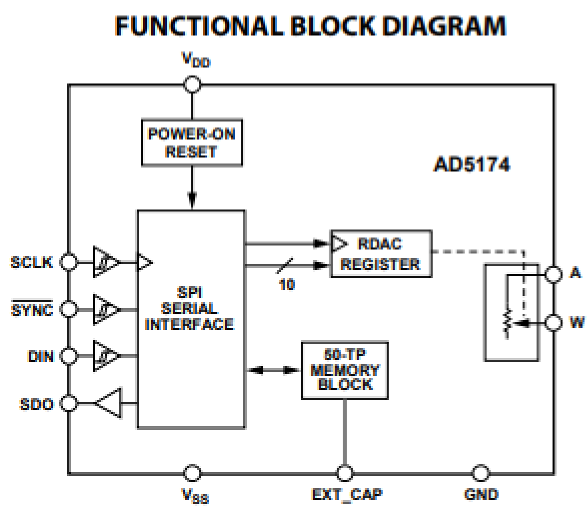

Figure 6: Functional Block Diagram of AD5174

VI. Schedule

<u>November:</u>

1. Awaiting shipment of EIS Board
2. Project Proposal Draft (11/6/18)
3. Project Presentation Draft (11/13/18)
4. Presentation Practice
5. Project Proposal Final (11/27/18)
6. Project Presentation Final (11/29/18)

<u>December:</u>

1. Website Development
2. Release Project Website (12/6/18)
3. Firmware Development

<u>January:</u>

1. Firmware Development

<u>February:</u>

1. Firmware Development
2. Self-Check (2/19/19)

<u>March:</u>

1. Firmware Development
2. Progress Evaluation (3/5/19)
3. Expo Registration (3/15/19)

<u>April:</u>

1. Firmware Development
2. Final Report Draft (4/5/19)
3. *Expo Abstract (4/5/19)*
4. Poster Print (4/11/19)
5. Project Conference Abstract (4/12/19)
6. *Expo Poster Setup (4/16/19)*
7. *Expo Poster Judging (4/17/19)*
8. Final Presentation Draft (4/23/19)

<u>May:</u>

1. Senior Project Conference (5/4/19)
2. All Deliverables (5/7/19)

VII. References

[1] R. Mingant, J. Bernard, V. Sauvant-Moynot, Novel state-of-health diagnostic method for Li-ion battery in service, In Applied Energy, Volume 183, 2016, Pages 390-398, ISSN 0306-2619, https://doi.org/10.1016/j.apenergy.2016.08.118.

[2] Wladislaw Waag, Stefan K¨abitz, and Dirk Uwe Sauer. Experimental investigation of the lithium-ion battery impedance characteristic at various conditions and aging states and its influence on the application. Applied Energy, 102(C):885–897, February 2013.

[3] Uwe Tr¨oltzsch, Olfa Kanoun, and Hans-Rolf Tr¨ankler. Characterizing aging effects of lithium ion batteries by impedance spectroscopy. Electrochimica Acta, 51(8-9):1664–1672, January 2006.

[4] Uwe Troeltzsch and Olfa Kanoun. Miniaturized Impedance Measurement System for Battery Diagnosis. Proceedings SENSOR 2009, Volume I, pages 251–256, 2009.

[5] Wang Li, Gen Wang Liu, and Fu He Yang. Design of Automatic Measurement System of Lithium Battery Electrochemical Impedance Spectroscopy Based on Microcomputer. Applied Mechanics and Materials, 241-244:259– 264, December 2012.

[6] F. Huet, "A review of impedance measurements for determination of the state-of-charge or state-of-health of secondary batteries," Journal of Power Sources, vol. 70, pp. 59-69, Jan 30 1998.

[7] D. A. Howey, P. D. Mitcheson, V. Yufit, G. J. Offer, and N. P. Brandon, "Online measurement of battery impedance using motor controller excitation," IEEE Trans. Veh. Technol., vol. 63, no. 6, pp. 2557–2566, Jul. 2014.

[8] S. E. Li, B. Wang, H. Peng, and X. Hu, "An electrochemistry-based impedance model for lithium-ion batteries," J. Power Sources, vol. 258, pp. 9–18, 2014.

[9] A. Christensen and A. Adebusuyi, "Using on-board electrochemical impedance spectroscopy in battery management systems," *2013 World Electric Vehicle Symposium and Exhibition (EVS27)*, Barcelona, 2013, pp. 1-7. doi: 10.1109/EVS.2013.6914969

[10] S.M.M. Alavi, C.R. Birkl, D.A. Howey, "Time-domain fitting of battery electrochemical impedance models," *Journal of Power Sources*, 28-Apr-2015.

[11] Haifeng Dai, Tianjiao Xu, Letao Zhu, Xuezhe Wei, Zechang Sun, Adaptive model parameter identification for large capacity Li-ion batteries on separated time scales, In Applied Energy, Volume 184, 2016, Pages 119-131, ISSN 0306-2619, https://doi.org/10.1016/j.apenergy.2016.10.020.

[12] Wen-Yeau Chang, "The State of Charge Estimating Methods for Battery: A Review," ISRN Applied Mathematics, vol. 2013, Article ID 953792, 7 pages, 2013. doi:10.1155/2013/953792

[13] Lauren M Marzocca, Terrill B Atwater, "Differential Capacity-Based Modeling for In-Use Battery Diagnostics, Prognostics, and Quality Assurance", US Army RDECOM, 2014, http://www.dtic.mil/get-tr-doc/pdf?AD=AD1018791

[14] Piret, Helene & Portier, B & Bacquet, S & Palmieri, M & Granjon, Pierre & Guillet, Nicolas & Cattin, V. (2015). EEVC -European Electric Vehicle Congress, “Key parameters design for online battery electrochemical impedance tracker”.

[15] H. C. Chen, S. R. Chou, H. C. Chen, S. L. Wu and L. R. Chen, "Fast Estimation of State of Charge for Lithium-Ion Battery," *2014 International Symposium on Computer, Consumer and Control*, Taichung, 2014, pp. 284-287. doi: 10.1109/IS3C.2014.82

[16] Hoja, Jerzy & Lentka, Grzegorz. (2009). Portable analyzer for impedance spectroscopy. 19th IMEKO World Congress 2009. 1.

[17] “FFT (Fast Fourier Transform) Waveform Analysis,” *FFT (Fast Fourier Transform) Waveform Analysis*. [Online]. Available: https://www.dataq.com/data-acquisition/general-education-tutorials/fft-fast-fourier-transform-waveform-analysis.html

[18] Xi Zhang, Jinling Lu and Xuan Zhou, "Transfer function establishment for Li-ion battery using improved P2D modeling methodology," *2016 IEEE 8th International Power Electronics and Motion Control Conference (IPEMC-ECCE Asia)*, Hefei, 2016, pp. 1378-1381.
doi: 10.1109/IPEMC.2016.7512491

[19] M. Frigo and S. G. Johnson, "The Design and Implementation of FFTW3," in *Proceedings of the IEEE*, vol. 93, no. 2, pp. 216-231, Feb. 2005. doi: 10.1109/JPROC.2004.840301

[20] X. Wang, X. Wei, H. Dai and Q. Wu, "State Estimation of Lithium Ion Battery Based on Electrochemical Impedance Spectroscopy with On-Board Impedance Measurement System," *2015 IEEE Vehicle Power and Propulsion Conference (VPPC)*, Montreal, QC, 2015, pp. 1-5.
doi: 10.1109/VPPC.2015.7353021

[21] E. Din, C. Schaef, K. Moffat and J. T. Stauth, "A Scalable Active Battery Management System With Embedded Real-Time Electrochemical Impedance Spectroscopy," in *IEEE Transactions on Power Electronics*, vol. 32, no. 7, pp. 5688-5698, July 2017. doi: 10.1109/TPEL.2016.2607519

[22] J. Gu, H. Yao, K. Wang, B. Parviz and B. Otis, "A 10μA on-chip electrochemical impedance spectroscopy system for wearables/implantables," *2014 IEEE Asian Solid-State Circuits Conference (A-SSCC)*, KaoHsiung, 2014, pp. 309-312. doi: 10.1109/ASSCC.2014.7008922

[23] Saeed Sepasi, Reza Ghorbani, Bor Yann Liaw, Inline state of health estimation of lithium-ion batteries using state of charge calculation, In Journal of Power Sources, Volume 299, 2015, Pages 246-254, ISSN 0378-7753, https://doi.org/10.1016/j.jpowsour.2015.08.091.

[24] Min-Hsuan Hung, Chang-Hua Lin, Liang-Cheng Lee, Chien-Ming Wang, State-of-charge and state-of-health estimation for lithium-ion batteries based on dynamic impedance technique, In Journal of Power Sources, Volume 268, 2014, Pages 861-873, ISSN 0378-7753,
https://doi.org/10.1016/j.jpowsour.2014.06.083.

[25] Yin Hua, Andrea Cordoba-Arenas, Nicholas Warner, Giorgio Rizzoni, A multi time-scale state-of-charge and state-of-health estimation framework using nonlinear predictive filter for lithium-ion battery pack with passive balance control, Journal of Power Sources, Volume 280, 15 April 2015, Pages 293-312, ISSN 0378-7753, https://doi.org/10.1016/j.jpowsour.2015.01.112.

[26] Andre, D., et al. “Characterization of High-Power Lithium-Ion Batteries by Electrochemical Impedance Spectroscopy. I. Experimental Investigation.” *Journal of Power Sources*, 12 Jan. 2011, www.elsevier.com/locate/jpowsour.

[27] Pulido, Yoana Fernandez. “Determination of Suitable Parameters for Battery Analysis by Electrochemical Impedance Spectroscopy.” *Journal of Power Sources*, University of Oviedo, 19 Apr. 2017, www.elsevier.com/locate/measurement.

[28] “AD5933,” 1 MSPS, 12-Bit Impedance Converter, Network Analyzer. [Online]. Available: https://www.analog.com/en/products/ad5933.html#product-overview. [Accessed: 06-Nov-2018]

[29] “AD5174,” Single-Channel, 1024-Position, Digital Rheostat with SPI interface and 50-TOP Memory. [Online]. Available: https://www.analog.com/en/products/ad5174.html [Accessed: 06-Nov-2018]